Theory of disorder-induced increase and degradation of superconducting T_c

D. Belitz

Department of Physics and Astronomy, University of Maryland, College Park, Maryland 20742

For a recent strong coupling theory for dirty superconductors, the leading disorder dependence of T_c is calculated exactly within a jellium model, and found to be linear in the resistivity ρ. Due to competition between attractive and repulsive effective electron-electron interactions, $dT_c/d\rho$ changes sign as a function of the clean-limit temperature T_c^0. This explains the experimental fact that low-T_c superconductors show an increase of T_c with disorder, while high-T_c materials show a T_c degradation. Analysis of experiments on many very different materials shows that this correlation is surprisingly well pronounced. Comparison of the model calculation with the experimental results yields satisfactory agreement.

I. INTRODUCTION

It has long been known that the superconducting T_c changes with the normal-state extrapolated residual resistivity ρ.[1-3] In these early experiments on simple metals, it was found that for weak coupling superconductors, T_c increases with increasing ρ, while the classical strong-coupling materials Pb and Hg showed no effect, and a slight decrease of T_c, respectively. At that time, these results were not understood, and also they later received little theoretical attention. In recent years, however, interest in effects of nonmagnetic disorder on T_c has been revived from the finding that in modern high-T_c materials, T_c decreases substantially with disorder,[4-8] a rather unfortunate effect from the practical point of view. However, the slope $dT_c/d\rho$ at small ρ is of the same order of magnitude for both T_c increase and degradation. This suggests underlying physical mechanisms of comparable strength, and calls for a theory capable of describing both, and the apparent transition between them.

Early theoretical attention concentrated on the spectacular difference between magnetic and nonmagnetic disorder. The relative insensitivity to the latter was shown[9] to be in accord with BCS theory, since Cooper pairs can be formed with arbitrary electron eigenstates, as long as time-reversal invariance holds. This fact is known as Anderson's theorem. Consequently, the observed disorder dependence can be looked for in the parameters of BCS theory, that is, the density of states (DOS), and the effective electron-electron (e-e) interaction. DOS effects provide the conventional explanation for the T_c degradation in transition metals and A-15 compounds. Thereby it is assumed that the DOS has a sharp peak near the Fermi energy, which is gradually smeared by disorder.[10] Analogously, for low-T_c A-15 materials such as Mo$_3$Ge, it is assumed that the Fermi energy lies between two peaks of the DOS. While there is sufficient evidence to tell that in some A-15 materials DOS effects do play a role, this is not sufficient to explain the observations. Apart from the fact that it definitely does not work for simple metals, it is unclear how strongly changes in single-particle properties will affect T_c.[11]

The second source of disorder dependence, namely the effective interaction, cannot be treated within BCS theory, where the interaction is a phenomenological parameter. Rather, one has to consider electron-phonon (e-ph) and Coulomb interactions on a microscopic level. If this could be done rigorously, DOS effects would be included as well. The first step in this direction was taken by Keck and Schmid.[12] Within Eliashberg theory, and neglecting Coulomb as well as DOS effects, these authors calculated the disorder dependence of the e-ph coupling λ. They obtained a disorder-induced rise of T_c, which for weak coupling is of the correct order of magnitude. For the T_c degradation in the strong-coupling regime, a number of explanations have been proposed, which mainly rely on disorder effects on the Coulomb pseudopotential.[11] Very recently it has been found that an even stronger effect comes from the normal self-energy.[13,14] The resulting strong-coupling equations have been discussed at length. In particular they were shown in Ref. 13(a) to contain as special cases the effects found before in Ref. 11. After some simplifications it was possible to find a generalized McMillan solution with disorder dependent e-ph coupling, Coulomb pseudopotential, and a normal self-energy parameter.[13(b)] Previous evaluation of these renormalizations in Ref. 13(b) neglected possible T_c enhancing effects. Therefore, comparison with experiment was restricted to the regime of strong coupling and large disorder, where these processes are indeed unimportant.

It is the purpose of the present paper to show that a more careful, though more restricted, evaluation of the theory developed in Ref. 13 yields an explanation of the observed change of sign of $dT_c/d\rho$ as a function of T_c^0. For this purpose, we concentrate on weak disorder, and evaluate the disorder renormalizations exactly to first order within a jellium model. While this model calculation neglects DOS effects, it explains the general trend of the data with reasonable parameters. In particular it shows that a change of sign of $dT_c/d\rho$ as a function of T_c^0 has to occur for a very general reason, namely competition between attractive and repulsive effective e-e interactions. This strongly suggests that the gross features of the experimental results can be understood within simple and

unspecific models, though details like band structures and phonon spectra will be important to quantitatively describe specific materials.

II. PERTURBATION THEORY FOR THE DISORDER DEPENDENCE OF T_c

A. T_c formula and disorder parameters

Our starting point is the generalized McMillan formula derived in Ref. 13:

$$T_c = \frac{\Theta_D}{1.45} \exp\left[\frac{-1.04(1+\tilde{\lambda}+Y')}{\tilde{\lambda}-\tilde{\mu}^*[1+0.62\tilde{\lambda}/(1+Y')]} \right] . \quad (2.1)$$

Here Θ_D is the Debye temperature and

$$\tilde{\lambda} = 2 \int_0^\infty (d\nu/\nu)\alpha^2 F(\nu) , \quad (2.2a)$$

$$\tilde{\mu}^* = U_c^W \left[1 + \frac{U_c^W}{1+Y'}\ln(E_B/k_B\Theta_D) \right]^{-1} , \quad (2.2b)$$

with

$$U_c^W = \sum_{q\neq 0} R_c^F(\mathbf{q})(\kappa^2/2N_F)/(q^2+\kappa^2) , \quad (2.2c)$$

and

$$Y' \equiv Y_c' + Y_p' = \sum_{q\neq 0}[\delta R_c^F(\mathbf{q}) - 2R_c^H(\mathbf{q})]\frac{\kappa^2/2N_F}{q^2+\kappa^2}$$
$$+ 4\int_0^\infty (d\nu/\nu)\alpha^2 F^H(\nu) . \quad (2.2d)$$

Here κ is the screening wave number, and N_F is the DOS per spin at the Fermi level. The generalized Eliashberg function $\alpha^2 F(\nu) = \alpha^2 F^F(\nu) + \alpha^2 F^H(\nu)$ consists of two contributions which stem from Fock- (F) and Hartree- (H)

type self-energy parts. They are defined as

$$\alpha^2 F^{F(H)}(\nu) = \sum_{q,b} R_b^{F(H)}(\mathbf{q})B_b(\mathbf{q},\nu) , \quad (2.3)$$

with phonon spectral function B_b for polarization branch b. Before we define the vertex functions $R_b^{F(H)}$, we briefly recall the physical meaning of the various quantities defined above. $\tilde{\lambda}$ and $\tilde{\mu}^*$ are disorder-dependent generalizations of the usual quantities λ and μ^*. In the case of $\tilde{\lambda}$, the disorder dependence is hidden in the vertex function entering the Eliashberg function, Eq. (2.3). A similar vertex function enters $\tilde{\mu}^*$ via U_c^W, which in the clean limit reduces to the usual parameter μ. All these terms arise from considering the contributions to standard strong-coupling theory in the presence of disorder. Additionally, there is the renormalization function Y', which enters $\tilde{\mu}^*$ as well as the T_c formula directly. Y' arises from the normal self-energy, which in standard Eliashberg theory only renormalizes the chemical potential, and hence can be neglected. In the presence of disorder, it is strongly energy dependent, and must be kept.

All this has been discussed at length in Ref. 13, where the vertex functions $R_b^{F,H}$ have been given in terms of Kubo correlation functions. For our present purposes, it is more convenient to express them in terms of retarded (+) and advanced (−) electronic Green's functions

$$\tilde{G}_{\mathbf{k},\mathbf{p}}^\pm(\omega) = \langle \mathbf{k} | \frac{1}{\omega - H \pm i0} | \mathbf{p} \rangle . \quad (2.4a)$$

Here H is the Hamiltonian for electrons moving in the disordered environment, without e-ph or e-e interactions. Impurity averaging yields

$$G_{\mathbf{k}}^\pm(\omega) \equiv \delta_{\mathbf{k},\mathbf{p}}G_{\mathbf{k},\mathbf{p}}^\pm(\omega) = \langle \tilde{G}_{\mathbf{k},\mathbf{p}}^\pm(\omega) \rangle_{av}$$
$$= \delta_{\mathbf{k},\mathbf{p}}[\omega - \epsilon_{\mathbf{k}} + \Sigma_{\mathbf{k}}^\pm(\omega)]^{-1} , \quad (2.4b)$$

where Σ is the self-energy due to disorder. The vertex functions R_i^J ($i=c,b$; $j=F,H$) read[13]

$$R_i^J(\mathbf{q}) = \frac{1}{2\pi^2 N_F} \sum_{\mathbf{k},\mathbf{p}} v_i^q(\mathbf{k})v_i^q(\mathbf{p}) \mathrm{Re}\langle G_{\mathbf{K}-\mathbf{Q}/2,\mathbf{P}-\mathbf{Q}/2}^+ G_{\mathbf{P}+\mathbf{Q}/2,\mathbf{K}+\mathbf{Q}/2}^- - (G^+\leftrightarrow G^-)\rangle_{av} , \quad (2.5a)$$

where $(\mathbf{K},\mathbf{P},\mathbf{Q})=(\mathbf{k},\mathbf{p},\mathbf{q})[(\mathbf{k}+\mathbf{p}-\mathbf{q})/2$, $(\mathbf{k}+\mathbf{p}+\mathbf{q})/2$, $\mathbf{k}-\mathbf{p}]$ for $J=F[H]$, and $G\equiv G(\omega=0)$. The vertices are

$$v_c^q(\mathbf{k}) = 1 , \quad (2.5b)$$

$$v_b^q(\mathbf{k}) = 3g_b[(\mathbf{k}\,\mathbf{q})(\mathbf{k}\,\mathbf{e}(\mathbf{q})) - \tfrac{1}{3}k_F^2(\mathbf{q}\,\mathbf{e}_b(\mathbf{q}))]/k_F^2 . \quad (2.5c)$$

Here $g_b = k_F^2/3m\sqrt{\rho_i}c_b$, with ρ_i and c_b denoting ion mass density, and sound velocity, respectively. $\mathbf{e}_b(\mathbf{q})$ is the phonon polarization vector. δR_c^F in Eq. (2.2d) denotes R_c^F with its clean-limit value subtracted. All other quantities have their usual meanings. The particular form of the e-ph vertex, Eq. (2.5c), stems from the particular e-ph interaction, the Tsuneto-Schmid model, used in Ref. 13. Notice that apart from this specific model for the vertex (the derivation of which uses a nearly free-electron picture), Eq. (2.5a) still contains band-structure effects via the Green's functions G. It is impossible to proceed analyti-

cally for nontrivial electron dispersion and electron impurity scattering. From now on, we therefore assume a jellium model with pointlike impurity scatterers: $\epsilon_{\mathbf{k}} = \hbar^2 k^2/2m$, $\Sigma_{\mathbf{k}}^\pm(\omega) = \pm i/2\tau$. τ is the scattering mean free time, which is related to the resistivity ρ by $\tau = (\tfrac{1}{2}\epsilon_F)/\hat{\rho}$, where $\hat{\rho} = \rho/\rho_M$ with Mott's resistivity $\rho_M = 3\pi^2\hbar/k_F e^2$.
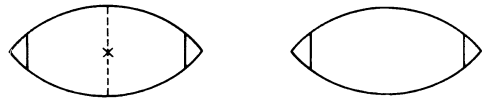

FIG. 1. Diagrammatic contributions up to first order in $\hat{\rho}$. Straight lines stand for G^+ or G^-. See text for further explanation.

B. Perturbation theory for the disorder parameters

It is now straightforward to calculate the R_i^j by means of standard diagrammatic technique.[15] We denote Green's functions by straight lines, the electron impurity

interaction by dashed lines, and the impurity density factor $1/(2N_F\tau)$ by a cross. The vertex $v_i^q(k)$ is denoted by a triangle. To first order in $1/\tau$ it is sufficient to consider the two diagrams shown in Fig. 1.

With the Coulomb vertex, Eq. (2.5b), we obtain

$$R_c^F(\mathbf{q}) = y^2\frac{\pi}{2q}\Theta(2k_F - q) + \bar{\rho}y^2\frac{k_F}{4q^2}\left[\pi^2\Theta(2k_F - q) + \ln^2\left|\frac{2k_F - q}{2k_F + q}\right|\left(-4 - \frac{4q^2}{q^2 - 4k_F^2}\right)\right] , \qquad (2.6a)$$

$$R_c^H(\mathbf{q}) = \bar{\rho}y^2\pi(k_F/q^2)\ln^2\left|\frac{2k_F - q}{2k_F + q}\right| , \qquad (2.6b)$$

where $y \equiv \kappa/2k_F$. Doing the integrals in Eqs. (2.2c) and (2.2d), we obtain

$$U_c^W = \mu + \delta\mu , \qquad (2.7a)$$

where

$$\mu = \frac{1}{2}y^2\ln(1 + 1/y^2) , \qquad (2.7b)$$

$$\delta\mu = \frac{1}{2}\bar{\rho}y\left[\pi\arctan\left[\frac{1}{y}\right] - \arctan^2\left[\frac{1}{y}\right] + \frac{1}{1+y^2} - 2\right] , \qquad (2.7c)$$

and

$$Y_c' = \bar{\rho}y\left[(\pi/2 - 2\pi^2)\arctan\left[\frac{1}{y}\right] \right.$$
$$\left. + (4\pi - 1/2)\arctan^2\left[\frac{1}{y}\right] + \frac{1/2}{1+y^2} - 1\right] . \qquad (2.8)$$

μ is the usual Coulomb potential,[16] and $\delta\mu$ is its first disorder correction. Y_c' is the first-order Coulomb contribution to the normal self-energy parameter.

Calculation of the e-ph vertex functions proceeds analogously, but is somewhat more cumbersome. After some algebra, we obtain

$$R_L^F(q) = g_L^2\frac{m}{2k_Fq}\Theta(2k_F - q)$$
$$- \bar{\rho}g_L^2\frac{m}{k_F^2}\frac{16 - \pi^2}{16\pi}(2k_F/q)^2[1 + O(q)] , \qquad (2.9a)$$

$$R_T^F(q) = \bar{\rho}g_T^2\frac{m}{k_F^2}\frac{3}{4\pi}(2k_F/q)^2[1 + O(q^2)] , \qquad (2.9b)$$

$$R_L^H(q) = \bar{\rho}g_L^2\frac{m}{k_F^2}64[1 + O(q^2)] , \qquad (2.9c)$$

There is no first-order contribution to R_T^H. In giving Eqs. (2.9), we have kept the leading q dependence only. The reason is that the effective e-ph interaction, Eq. (2.5c), Tsuneto-Schmid model, is valid for long-wavelength phonons only. For larger q, no e-ph interaction is available. We follow the common practice to extrapolate the small-q behavior to all q.

In order to calculate α^2F, Eq. (2.3), we still need to know the phonon spectrum. For our model calculation, we take a simple Debye spectrum:

$$B_b(q,\nu) = \frac{1}{2}c_bq\delta(\nu - c_bq)\Theta(\omega_D - \nu) . \qquad (2.10)$$

This is compatible with our small-q e-ph interaction. It is now elementary to calculate $\tilde{\lambda}$ and Y' from Eqs. (2.2a) and (2.2d):

$$\tilde{\lambda} \equiv \lambda + \delta\lambda = \lambda + \bar{\rho}\lambda[12(c_L/c_T)^2 - 8 + \pi^2/2]/\pi x_D , \qquad (2.11)$$

$$Y' = \bar{\rho}\left\{y\left[\frac{3}{2}\text{arctg}^2\left[\frac{1}{y}\right] - \frac{\pi}{2}\text{arctg}\left[\frac{1}{y}\right] + \frac{1/2}{1+y^2} - 1\right]\right.$$
$$\left. + \frac{1024}{9}x_D\lambda\right\} . \qquad (2.12)$$

Here $\lambda = \tilde{\lambda}(\bar{\rho} = 0) = g_L^2N_Fx_D^2$, and $x_D = q_D/2k_F$.

From Eqs. (2.7), (2.12), and (2.1), we now obtain the following result for the first-order correction $\delta t \equiv (T_c - T_c^0)/T_c^0$ to the critical temperature:

$$\delta t = \frac{-1.04(1+\lambda)}{[\lambda - \mu^*(1+0.62\lambda)]^2}\left\{\frac{\delta\lambda + Y'}{1+\lambda}[\lambda - \mu^*(1+0.62\lambda)] + \mu^*(1+0.62\lambda)\left[\delta\mu^*/\mu^* + \frac{0.62\lambda}{1+0.62\lambda}(\delta\lambda/\lambda - Y')\right] - \delta\lambda\right\} . \qquad (2.13)$$

Here λ is the clean-limit parameter given above, and $\mu^* = \bar{\mu}^*(\bar{\rho} = 0) = \mu/[1 + \mu\ln(E_B/k_B\Theta_D)]$. The corrections $\delta\lambda$ and Y' are given by Eqs. (2.11), and (2.12), respectively. The correction to the Coulomb pseudopotential reads

$$\delta\mu^* = \mu^*[\delta\mu/\mu + \mu Y'\ln(E_B/k_B\Theta_D)]/[1 + \mu\ln(E_B/k_B\Theta_D)] , \qquad (2.14)$$

with $\delta\mu$ from Eq. (2.7c).

Within the jellium and Debye models for electrons and phonons, respectively, Eq. (2.13) constitutes the exact first-order correction to T_c for the theory developed in Ref. 13. In the remaining part of this paper we discuss this result.

III. RESULTS AND DISCUSSION

A. General features of $dT_c/d\rho$

Let us start with a general discussion of Eq. (2.13). We have found the leading disorder correction to T_c to be linear in ρ. It is clear that this feature will not be changed by considering more realistic models. Of the approximate calculations done so far, the present author obtained a linear dependence (albeit with different prefactor) in Refs. 17 and 13. On the other hand, in Ref. 18 a quadratic behavior, $\delta t \propto \rho^2$, has been predicted. The present exact calculation shows that this feature of the result of Ref. 18 is incorrect.[19] The reason lies in an improper handling of the density propagator, as has been discussed in Ref. 17. The linear behavior also compares favorably with experiments. We will come back to this in Sec. III B.

To see the gross behavior of $dT_c/d\rho$ as a function of the e-ph coupling we neglect the Coulomb repulsion for a while: $\mu^*=0$. Then Eq. (2.13) simplifies to
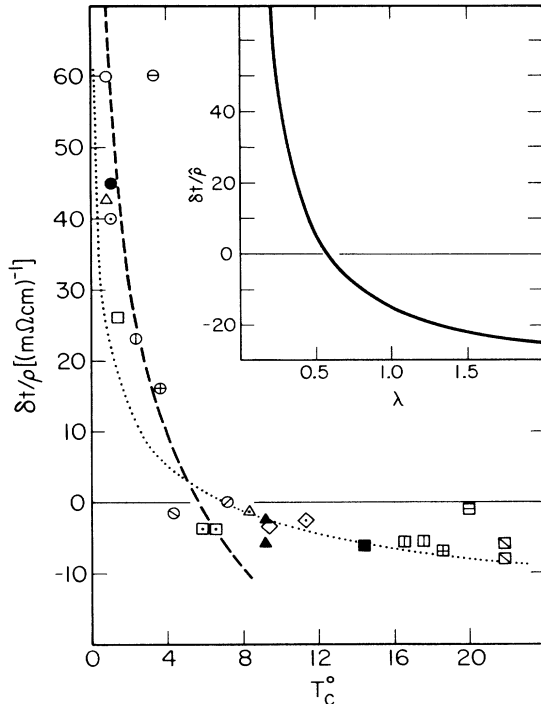

FIG. 2. $\delta t/\rho$ plotted versus T_c^0 according to the data shown in Table I. Estimated uncertainties of $\delta t/\rho$ are not shown. Symbols are the same as those in Table I. Dashed (dotted) lines are the theoretical result, Eq. (2.13), with $y=0.5(1.0)$; $\ln(E_B/k_B\Theta_D)=5(2)$; $x_D=0.30(0.32)$; $(c_L/c_T)^2=1.8(1.8)$; $\Theta_D=200(400)K$; $\rho_M=750(2400)$ $\mu\Omega$cm. The inset shows the simplified formula, Eq. (3.1), for $x_D=0.30$ and $(c_L/c_T)^2=1.8$.

$$\delta t/\hat{\rho}=\frac{1.04}{\lambda}(a-b\lambda)\ ,\qquad (3.1)$$

where $a=\delta\lambda/\hat{\rho}\lambda$ and $b=Y'(y=0)/\hat{\rho}=1024x_D/9$. This function is plotted in the inset of Fig. 2 of $x_D=0.30$. We see that for small λ, δt is positive and proportional to $1/\lambda$. For large λ, δt is negative, and saturates at $-1.04b$. Since λ is a measure of T_c, we expect a positive correction with a strong-T_c dependence at small T_c, and a negative correction with a weak-T_c dependence at large T_c. This is exactly what is found in experiment, as we will see.

B. Experimental results and comparison with theory

In Table I, we give superconductivity parameters and the value of $\delta t/\rho$ for a variety of materials. For λ, tunneling results are given whenever available. If no reference is given, λ and μ^* have been obtained by McMillan's semiempirical method.[20] The column $\delta t/\rho$ requires a few remarks. (i) For all quoted experiments where there are sufficient data to judge it, the small-ρ behavior of T_c can be reasonably interpreted as linear. Bending et al.[8] found the behavior of V-Ga to be quadratic, but a linear fit to their data is of equal quality. (ii) It is well-known that at very small resistivities (typically $\rho \lesssim 1$ $\mu\Omega$cm) there is a sharp initial drop of T_c. This is equally true for simple metals,[21] and for A-15 materials.[22] This phenomenon has been interpreted by Anderson[9] as smearing of anisotropies before the "dirty limit" is reached, where $\hbar/\tau$ is larger than the gap, and the behavior of T_c is much more gradual. This phenomenon is, of course, not included in the present calculation. To see the physical effects we are looking for, we therefore have to ignore this rapid initial variation of T_c in extracting $\delta t/\rho$ from the data. In the experiments quoted in Table I, the initial drop is not visible anyway. (iii) In some of the experiments, only two points of T_c versus ρ have been obtained. In others the data scatter considerably. The estimated resulting uncertainties are given in the table. If there is no uncertainty shown, we have found no reasonable way to estimate it. (iv) There are many more experiments in the literature, where δt is given as a function of radiation dose, or some other measure of disorder. It should be stressed that for a theoretical analysis the resistivity, though harder to measure, is the only valuable disorder parameter, since it is the only one directly related to microscopic quantities.

From Table I it is already conspicuous that there is a correlation between $\delta t/\rho$ and λ or T_c^0. This is most pronounced if $\delta t/\rho$ is plotted versus T_c^0, as is done in Fig. 2. The plot shows a steep low-T_c branch, which is mainly made up by simple metals, and a flat high-T_c branch, which mainly consists of A-15 materials. Transition metals and their compounds are present in both regions, and the low-T_c A-15 Mo$_3$Ge fits nicely into the low-T_c branch. It is surprising how well the correlation is pronounced, since the plot contains 20 different superconductors belonging to four different classes of materials.

It is already clear from the discussion given in Sec. III A that our theoretical result shares the main features with the experimentally observed correlation. The remaining questions are of quantitative nature. Of course our model calculation is not capable of producing $\delta t/\rho$

TABLE I. Superconductivity parameters, and disorder dependence of T_c, for various materials. A-15 materials have been denoted by M_3X, even if the actual materials were not stoichiometric compounds. Symbols for the different materials are those used in Fig. 1. See text for further explanation.

		T_c^0 (K)	$\delta t/\rho(10^5\Omega^{-1}m^{-1})$	$\bar\omega_{\log}$ (K)	Θ_D (K)	λ	μ^*
Zn	○	0.85[a]	60±10[b]		309[a]	0.38[a]	0.12[a]
Ga	⊙	1.08[a]	40±5[b]		325[a]	0.40[a]	0.102
Al	●	1.16[a]	190+20[b]		428[a]	0.38[a]	0.098
			45±5[c]				
Tl	⊕	2.38[a]		52[c]	79[a]	0.795[c]	0.111[c]
			23±5[d]				
In	⊖	3.40[a]	60±5[b,f]	68[c]	112[a]	0.805[c]	0.097[c]
Sn	⊕	3.72[a]	16±4[b,f]	99[c]	112[a]	0.72[c]	0.092[c]
Hg	⊘	4.16[a]	−1.50±0.2[b]	29[c]	72[a]	1.6[c]	0.098[c]
Pb	⊘	7.19[a]	0[b]	56[c]	105[a]	1.55[c]	0.105[c]
Mo	△	0.92[a]	43[g,h]	236[c]	460[a]	0.41[a]	0.09[a]
MoRuP	△	8.4[i]	−1±0.5[i]				
			−5.7±2.3[h]				
Nb	▲	9.22[a]		166[c]	277[a]	0.93[h]	0.1[h]
			−2.3±1.5[j]				
Mo₃Ge	□	1.42[k]	26±3[k]		435[k]	0.48	0.15
		5.8[l]					
V₃Ge	⊡		−3.8[j]		470[l]	0.67[l]	0.17[l]
		6.5[j]					
V₃Ga	■	14.3[l]	−6.2±1[m]		399[l]	1.12[l]	0.21[l]
		16.5[l,n]			498[l]		
V₃Si	田		−5.7±1.2[j,n,o]			1.03[l]	0.20[l]
		17.5[o]			520[a]		
Nb₃Sn	⊟	17.9[l]	−1±1[n,p]	125[c]	308[l]	1.80[l]	0.18[l]
Nb₃Al	⊞	18.5[l]	−7±2[q]		370[l]	1.7[l]	0.16[l]
			−6.1±1[o,p]				
Nb₃Ge	⊠	21.8[l]			302[l]	1.64[l]	0.15[l]
			−7.8±1.3[j]				
ErRh₄B₄	◇	9.4[o,p]	−3.6[o,p]				
LuRh₄B₄	◇	11.3[o]	−2.5[o]				

[a]See Ref. 20.
[b]See Ref. 1.
[c]See Ref. 25.
[d]See Ref. 3.
[e]See Ref. 26.
[f]See Ref. 2.
[g]See Ref. 27.
[h]See Ref. 28.
[i]See Ref. 29.
[j]See Ref. 30.
[k]See Ref. 31.
[l]See Ref. 32.
[m]See Ref. 8.
[n]See Ref. 6.
[o]See Ref. 7.
[p]See Ref. 4.
[q]See Ref. 5.

quantitatively for a given material, and all we can hope is to get the general trend correct with reasonable parameters. For simple metals, we choose $y=0.5$ and $\ln(E_B/k_B\Theta_D)=5$ (this yields $\mu^*=0.10$), $x_D=0.30$, $(c_L/c_T)^2=1.8$, $\Theta_D=200$ K, and $\rho_M=750$ $\mu\Omega$cm as typical parameters. This yields the dashed curve in Fig. 2. For transition metals and A-15 materials, μ^* and Θ_D are generally much larger, and we choose $y=1.0$, $\ln(E_B/k_B\Theta_D)=2$, $x_D=0.32$, $(c_L/c_T)^2=1.8$, $\Theta_D=400$ K. With $\rho_M=2400$ $\mu\Omega$cm, we obtain the dotted curve in Fig. 2. Notice that ρ_M sets only the scale for the vertical axis, and that for the high-T_c data we have to choose a rather high value for ρ_M to get the correct scale. A possible sim-

ple explanation for this is the following. In narrow-band materials, our jellium model is, of course, inadequate. The principal effect of the narrow band, however, will be a decrease of the conductivity scale, and hence an increase of the effective ρ_M. The resistivity scale for A-15 materials chosen here differs from our previous estimates.[13,17] At present we do not know which is more realistic. We conclude that the present theory describes well the general behavior of $dT_c/d\rho$ as a function of T_c^0 with reasonable parameters.

A remarkable feature of $T_c(\rho)$ is the very steep characteristic at low T_c. As a consequence, very small variations of phonon parameters (particularly x_D) result in

large changes of $\delta t/\rho$. This may explain the large differences between different samples of granular aluminum. Differences in the sample preparation will certainly lead to small variations in the phonon parameters, to which $\delta t/\rho$ is very sensitive because of the small T_c^0.

C. Discussion

We finally discuss the physics leading to the behavior described above. Again we first neglect the Coulomb interaction, and look at Eq. (3.1). The behavior of $\delta t/\hat{\rho}$ is clearly determined by competition between T_c enhancing effects described by $\delta\lambda$, and the T_c decreasing effects described by Y'.

Our result for $\delta\lambda$, Eq. (2.11), is identical to the one obtained before by Keck and Schmid.[12] Its net effect of increasing T_c comes from the disorder-induced onset of coupling to transverse phonons, Eq. (2.9b), which overcompensates a decrease in the coupling to longitudinal phonons. The physics of this mechanism, its connection to the well-known behavior of the sound attenuation coefficient, and the experimental status have been discussed elsewhere very recently,[23] so we do not have to repeat this.

Y' stems from the normal self-energy $S(\epsilon,\omega)$. In standard superconductivity theory, S is independent of both frequency and energy, and can be neglected. In the presence of disorder, S develops a peculiar energy dependence, and has to be kept. This is well-known for the Coulomb contribution to S, which gives rise to an anomaly in the normal-state DOS discovered by Altshuler and Aronov.[24] In Ref. 13 it was shown that there is also a phonon contribution to this effect. This was to be expected, since the Altshuler-Aronov effect clearly does not depend on the nature of the effective e-e interaction. It was also shown in Ref. 13 that the Hartree-type self-energy contributions (which had been neglected in Ref. 24) are important, and lead to a reinforcement of the repulsive Coulomb effect. So we end up with a mechanism which decreases the one-particle spectrum, and whose phonon contribution is proportional to λ. This is reflected in the parameter Y', Eq. (2.12), which is clearly adverse to superconductivity. The fact that both T_c-enhancing and T_c-decreasing mechanisms depend on λ is crucial for our explanation of the $\delta t - T_c$ correlation. The λ dependence of Y' could be checked directly by measuring the tunneling DOS. The normal self-energy of Ref. 13, leading to the Y' given in Eq. (2.12), also implies an Altshuler-Aronov anomaly of the tunneling DOS

$$N(\epsilon) = N(0)(1 + \sqrt{\epsilon/\Delta_c}) , \tag{3.2a}$$

with a correlation gap

$$\Delta_c = \frac{16}{27}\epsilon_F[\mu(\zeta - 3) + 4\lambda]^{-2}\hat{\rho}^{-3} , \tag{3.2b}$$

where $\zeta \equiv (1/y)\arctan(1/y)/\ln(1 + 1/y^2)$. Equations (3.2a) and (3.2b) predict a λ dependence of the correlation gap. For all superconductors, $|\mu(\zeta - 3)| \ll 4\lambda$, so that essentially $\Delta_c \propto \lambda^{-2}$, which should not be hard to check experimentally. For instance, Eqs. (3.2) predict for lead an effect which is one order of magnitude smaller than the one found in aluminum.[25] One has to keep in mind, however, that Eqs. (3.2) are valid only for $\hat{\rho} \ll 1$. For $\hat{\rho} \gtrsim 1$, experiment[25] yields a $\hat{\rho}^{-2}$ dependence. Nevertheless, Eq. (3.2b) gives the correct value for aluminum at $\hat{\rho} = 1$. It would be extremely interesting to repeat this experiment with Al and Pb samples of comparable resistivities.

If we now conclude the Coulomb pseudopotential, we go from Eq. (3.1) to Eq. (2.13). The Coulomb potential μ itself is affected by the disorder, Eq. (2.7c). Because of the structure of μ^*, however, this has little effect. An additional effect comes from the term in square brackets multiplying $\bar{\mu}^*$ in Eq. (2.1). Again this has little effect, since both λ and Y' rise with the resistivity. We conclude that the essential physics (for small disorder) is already included in Eq. (3.1). The Coulomb pseudopotential is important to get realistic numbers, however.

We finally come back to Fig. 2. As we have stressed before, the present model calculation is not adequate for either transition metals or A-15 materials. Also, for simple metals there are serious deficiencies like the Debye phonon spectrum, and the neglect of umklapp processes. Nevertheless, both the well-pronounced experimental correlation between $\delta t/\rho$ and T_c^0 for a large variety of materials, and the fact that this correlation is well explained by the theory, strongly suggest the following view. The general behavior of T_c as a function of ρ at small ρ, that is the sign of $\delta t/\rho$ and its approximate value, is independent of the details of the material, and governed by very general processes affecting the effective e-e interaction. Material specific properties like band structure and phonon spectra will be important to understand a given material quantitatively, but are not needed to understand the general trend of all superconducting metals.[1-8,25-32] For instance, there is the question of why $\delta t/\rho$ of Nb_3Sn is so small, and why that of In is so large. There also remain many questions at larger resistivities. The present theory cannot explain (nor is it designed to do so) why T_c of Al and Ga rises substantially up to $\rho > 200\ \mu\Omega$cm, while that of Zn and Sn saturates at $\rho \simeq 20\ \mu\Omega$cm. All these questions require more theoretical work.

[1]W. Buckel and R. Hilsch, Z. Phys. **138**, 109 (1954).

[2]G. Bergmann, Z. Phys. **228**, 25 (1969).

[3]A. Comberg, S. Ewert, and G. Bergmann, Z. Phys. **271**, 317 (1974).

[4]J. M. Rowell, R. C. Dynes, and P. H. Schmidt, in *Superconductivity in d- and f-band Metals,* edited by H. Suhl and M. B. Maple (Academic, New York, 1980).

[5]A. K. Ghosh and M. Strongin, in *Superconducting in d- and f-band Metals,* Ref. 4.

[6]T. P. Orlando, E. J. McNiff, S. Foner, and M. R. Beasley, Phys. Rev. B **19**, 4545 (1979).

[7]J. M. Rowell and R. C. Dynes (unpublished).

[8]S. J. Bending, M. R. Beasley, and C. C. Tsuei, Phys. Rev. B **30**, 6342 (1984).

[9]P. W. Anderson, J. Phys. Chem. Sol. **11**, 26 (1959).

[10]L. R. Testardi and L. F. Mattheiss, Phys. Rev. Lett. **41**, 1612 (1978).

[11]See the discussion by P. W. Anderson, K. A. Muttalib, and T. V. Ramakrishnan, Phys. Rev. B **28**, 117 (1983); H. Gutfreund, M. Weger, and O. Entin-Wohlman, *ibid.* **31**, 606 (1985); O. Entin-Wohlman, H. Gutfreund, and M. Weger, J. Phys. F **16**, 1545 (1986).

[12]B. Keck and A. Schmid, J. Low Temp. Phys. **24**, 611 (1976).

[13](a) D. Belitz, Phys. Rev. B **35**, 1636 (1987); (b) D. Belitz, Phys. Rev. B **35**, 1651 (1987).

[14]The importance of the normal self-energy has been noticed independently of Ref. 13 by D. A. Browne, K. Levin, and K. A. Muttalib, Phys. Rev. Lett. **58**, 156 (1987).

[15]A. A. Abrikosov, L. P. Gorkov, and I. E. Dzyaloshinskii, *Methods of Quantum Field Theory in Statistical Physics* (Prentice-Hall, Englewood Cliffs, 1963).

[16]P. Morel and P. W. Anderson, Phys. Rev. **125**, 1263 (1962).

[17]D. Belitz, J. Phys. F **15**, 2315 (1985).

[18]S. Maekawa, H. Ebisawa, and H. Fukuyama, J. Phys. Soc. Jpn. **53**, 2681 (1984).

[19]This conclusion is not model dependent. Evaluation of the diagrams in Ref. 18 exactly to leading order in ρ also yields a linear result.

[20]W. L. McMillan, Phys. Rev. **167**, 166 (1968).

[21]E. A. Lynton, B. Serin, and M. Zucker, J. Phys. Chem. Sol. **3**, 165 (1957).

[22]R. Schneider, G. Linker, O. Meyer, M. Kraatz, in *Proceedings of LT-17,* edited by U. Eckern, A. Schmid, W. Weber, and H. Wühl (North Holland, Amsterdam, 1984).

[23]D. Belitz, Phys. Rev. B (to be published).

[24]B. L. Altshuler, and A. G. Aronov, Solid State Commun. **30**, 115 (1979).

[25]R. C. Dynes and J. P. Garno, Phys. Rev. Lett. **46**, 137 (1981).

[26]P. B. Allen and R. C. Dynes, Phys. Rev. B **12**, 905 (1975).

[27]M. Gurvitch, Phys. Rev. B **28**, 544 (1983).

[28]D. B. Kimhi and T. H. Geballe, Phys. Rev. Lett. **45**, 1039 (1980).

[29]W. L. Johnson, J. Appl. Phys. **50**, 1557 (1979).

[30]L. R. Testardi, J. M. Poate, and H. J. Levinstein, Phys. Rev. B **15**, 2570 (1977).

[31]M. Gurvitch, A. K. Ghosh, B. L. Gyorffy, H. Lutz, O. F. Kammerer, J. S. Rosner, and M. Strongin, Phys. Rev. Lett. **41**, 1616 (1978).

[32]H. B. Radousky, T. Jarlborg, G. S. Knapp, and A. J. Freeman, Phys. Rev. B **26**, 1208 (1982).